Measurements of conversion coefficients using a Si(Li) detector

V. Horvat, J.C. Hardy, N. Nica, and V.E. Iacob

As part of our program to make precise measurements of internal conversion coefficients (ICCs) [1], we neutron-activated a natural ruthenium sample to produce ^{103}Ru [2]. The β decay of ^{103}Ru populates a 40-keV isomeric state in ^{103}Rh, which decays by an *E*3 transition, whose ICC we seek to measure. The low-energy region of the photon spectrum from ^{103}Ru decay is dominated by the *K* x rays from rhodium, the intensity of which we must determine, but there is also a weak but significant contribution from ruthenium *K* x rays excited by fluorescence of the activated-source material. Unfortunately the *K* x rays of ruthenium and rhodium could not be resolved in our well-calibrated HPGe detector, so we also recorded the spectrum in a Si(Li) detector.

A portion of the Si(Li) spectrum containing peaks due to both ruthenium and rhodium *K* x rays is shown in Figure 1 by the blue line. The red (green) lines indicate the expected peak centroids and relative intensities of rhodium (ruthenium) peaks. It was found that the observed number of ruthenium *K* x rays amounts to 3.1% of the observed number of rhodium *K* x rays.

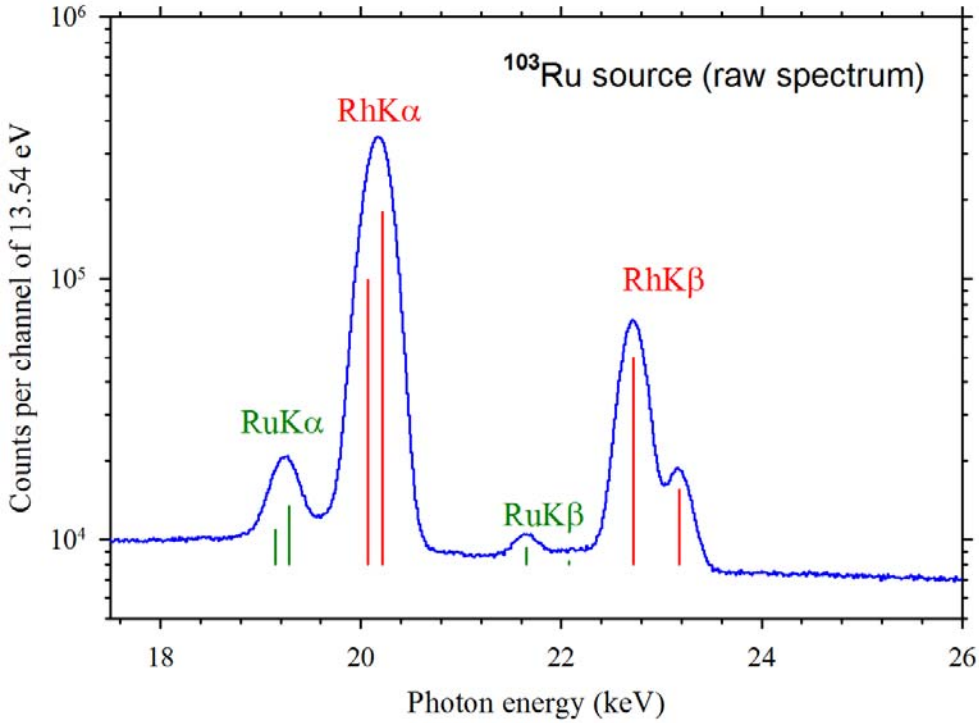

FIG. 1. Spectrum of x rays from the ^{103}Ru source measured using our Si(Li) detector.

Since there is no overlap between the peaks in the K_α group and those in the K_β group, the two groups were analyzed separately in order to simplify modeling of the peaks and the background and to

make the model more realistic. Specifically, the background in each group was modeled with an exponential decay curve using only two parameters, whose best values were adjusted based on visual inspection and then fixed. This was done in order to estimate the background with good accuracy and to make sure that the result is not affected by the peak-fitting procedure. The peaks were initially modeled with single Gaussian functions, but this model was subsequently refined.

In the peak-fitting procedure, the intensity of the peak due to Rh $K_{\alpha 2}$ x rays was fixed relative to the intensity of the peak due to Rh $K_{\alpha 1}$ x rays based on the calculated intensity ratio [3]. The same was done for the two peaks in the Ru K_{α} doublet. This way the centroids and intensities of the four peaks in each group were described by only three variable parameters. In the K_{α} group those were the Rh $K_{\alpha 1}$ and Ru $K_{\alpha 1}$ peak intensities and the Rh $K_{\alpha 1}$ peak centroid; while the variable parameters in the K_{β} group were the Rh $K_{\beta 1}$ and Ru $K_{\beta 1}$ peak intensities and the Rh $K_{\beta 1}$ peak centroid. The widths of the peaks were defined well enough to be fitted individually.

This simple model had to be adjusted in order to account for relatively small tails that were observed on the low-energy sides of the peaks. Contributions from these tails were evident in the plots of the fit residuals. It was found that these contributions could be described well with Gaussian functions having a lower centroid and an increased width compared to those describing the principal contributions to the peaks. In order to have a consistent peak profile for all peaks, we fixed the ratio of secondary-to-primary Gaussian areas for all peaks. The best-fit value of this fraction was found to be 4.2%. Also, the centroid energy difference between the secondary and primary peaks was taken to be proportional to the corresponding photon energy. For Rh $K_{\alpha 1}$, at 20.2163(1) keV [3], the best-fit value of the difference was found to be 190 eV.

Finally, for the Rh $K_{\alpha 1}$ peak, the best-fit widths (standard deviations) of the primary and the secondary Gaussian were found to be 115 eV and 331 eV, respectively. We then imposed the same ratio

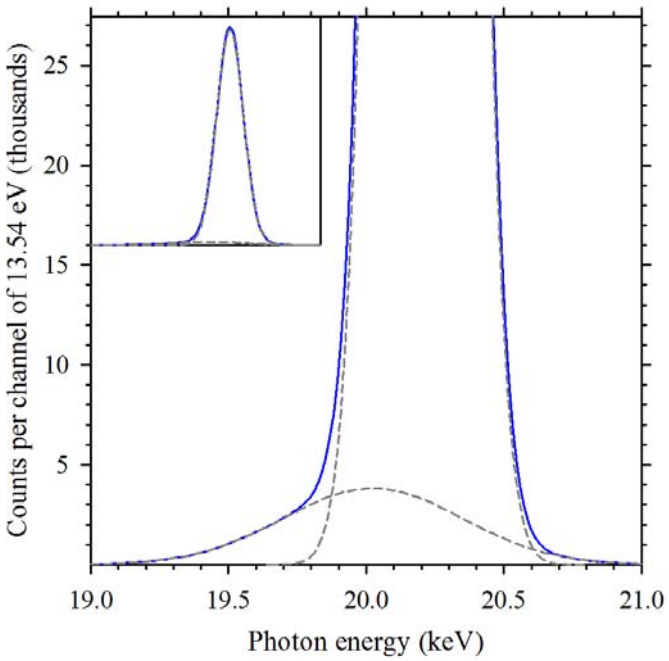

FIG. 2. Model of the fitted peak profile applied to the RhKα1 peak.

of widths when fitting the remaining peaks, so that only one variable parameter was used to describe the widths of all secondary Gaussians. This was implemented in a procedure that involved several iterations, and yielded the values given above.

Figure 2 shows the modeled shape of the Rh $K_{\alpha 1}$ peak. Note that the vertical scale covers only 10% of the full range in order to enhance the details. The full coverage is shown in the insert.

Figure 3 shows the energy region containing the K_{α} group of peaks. The blue dots with error bars are the measured data with the fitted *primary* Gaussians and background subtracted. The dashed grey lines represent the individual *secondary* Gaussians, with their sum being the solid red line. In addition, the solid green line shows the full spectrum as predicted by CYLTRAN calculations folded with the appropriate instrumental resolution function (assumed to be Gaussian). Evidently, the red line describes the data extremely well down to the energy at which CYLTRAN predicts a substantial contribution from Compton scattering, which was not included in our model. It is obvious from Figure 3 that inclusion of Compton scattering in the model would lead to a satisfactory description of the data over the entire region of interest. However, we did not try this, not only because it would add to the complexity of the analysis, but also because it was unnecessary: The peak areas are not influenced by the Compton scattering.

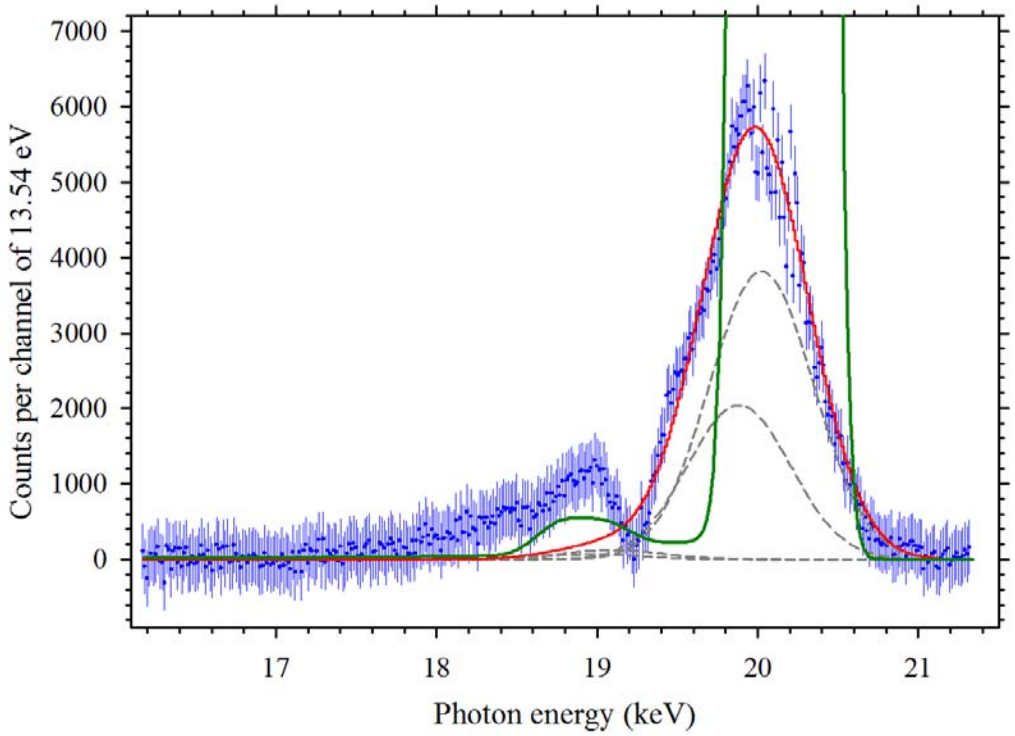

FIG. 3. Portion of the measured spectrum containing the K_{α} group of peaks, showing data from which we subtracted the fitted primary Gaussians and the background. Also shown are the fitted secondary Gaussians (dashed grey lines) and their sum (solid red line). In addition, the solid green line shows the spectrum predicted by CYLTRAN calculations folded with the appropriate instrumental resolution function (assumed to be Gaussian).

The peak due to the ^{103}Ru gamma ray at 39.757 keV [4] did not have a low-energy tail; therefore it was fitted with a single Gaussian function. The result is illustrated in Figure 4.

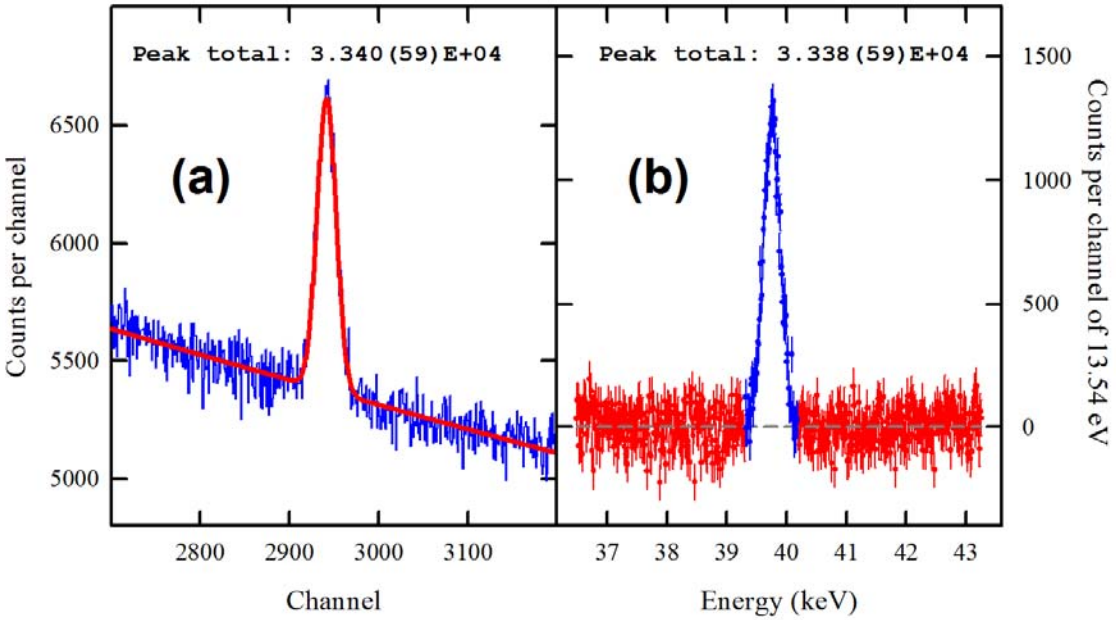

FIG. 4. Region of the measured spectrum containing the peak due to the ^{103}Ru gamma ray at 39.757 keV and the results of the analysis. The spectrum shown on the right is background-subtracted.

Analysis of the measured spectrum produced the results shown in Table I, for which we used Si(Li)-detector efficiencies as calculated with the CYLTRAN code [5], based on the nominal detector geometry, the actual ^{103}Ru source size, and the actual source position. Note that the number of Ru *K* x rays includes those resulting from internal conversion of all the other ^{103}Ru gamma rays, as well as those created in the decay of all other Ru isotopes present in the source.

Table I. Results of the analysis of the measured spectrum of x rays and gamma rays from the ^{103}Ru source.

Component	Efficiency-corrected number of events
RhKα	4.1290(19) E8
RhKβ1'	7.0792(96) E7
RhKβ2'	1.2766(59) E7
Total RhKx	4.964(24) E8
Rhγ(39.757 keV)	4.216(74) E6

[1] J.C. Hardy *et al.*, *Progress in Research*, Cyclotron Institute, Texas A&M University (2017-2018), p. I-25.
[2] N. Nica *et al.*, *Progress in Research*, Cyclotron Institute, Texas A&M University (2017-2018), p. I-28.
[3] E. Schönfeld and G. Rodloff, PTB Report: PTB-6.11-1999-1 (1999).
[4] http://nucleardata.nuclear.lu.se/toi/, accessed on 05/08/2018.
[5] J.A. Halbleib, R.P. Kensek, T.A. Mehlhorn, G.D. Valdez, S.M. Seltzer, and M.J. Berger, CYLTRAN 3.0, Sandia National Labs (Albuquerque, NM), Report SAND91-1634 (1992).